Fracture Energies and Tensile Strength of an EPDM/PP Thermoplastic Elastomer

CHI WANG,* C.-I. CHANG

Department of Chemical Engineering, National Cheng Kung University, Tainan, 701-01, Taiwan

Received 14 September 1998; accepted 1 July 1999

ABSTRACT: Measurements of the tear strength of EPDM/PP thermoplastic elastomers (EPDM/PP TPEs, Santoprene 201-87) were carried out at various rates and temperatures. In addition, a cutting technique developed recently was adopted to measure the fracture energy in a process where a well-controlled geometry of the crack tip was obtained. Results show that the EPDM/PP TPEs possess a relatively high tear strength of 10.40 ± 0.94 kJ/m^2 at room temperature. Furthermore, good tear strength is still preserved, about 1.87 ± 0.38 kJ/m^2, at 150°C, where some PP crystals are melted and start to flow. In contrast, the intrinsic strength of EPDM/PP TPEs determined from a cutting test is varied slightly, 700–1000 J/m^2, over a wide range of temperatures and rates. A comparison of the fracture energy measured by tearing and cutting tests is provided and discussed. The energy density per unit volume of EPDM/PP TPEs determined from the cutting test is 9.7 GJ/m^3, which is about twice larger than that for the rupture of C—C bonds at room temperature. It is suggested that plastic yielding is a more effective process to enhance the toughness than is simply viscoelastic motion.
 J Appl Polym Sci 75: 1033–1044, 2000

Key words: EPDM/PP thermoplastic elastomers; fracture energy; tear test; cutting test

INTRODUCTION

For decades, much attention has been paid to thermoplastic elastomers (TPEs) from practical and scientific points of view. Due to their unique microstructure, TPEs are noted for their attractive elastic properties at room temperature, their flowability at high temperatures, and a remelting process for recycle use. The elastic performance is attributed to the physical crosslinks (domain formation) resulting from the segregation of different phases. There have been many studies of structural changes which accompany the deformation of TPEs,[1–5] especially the styrene–butadiene–styrene (SBS) triblock copolymers. Many researchers combined the observation of microdomain deformation with structural studies from both small-angle X-ray scattering and transmission electron microscopy (TEM). Emphasis has been put on the stress–strain response and its relation to the microdomain deformation. On the other hand, systematic investigation of the fracture energy and fracture mechanism have received much less attention. In previous articles,[6,7] we explored the fracture energies of SBS block copolymers at various temperatures and rates.

It is generally recognized that polypropylene (PP) possesses good mechanical properties at room temperature. However, due to a relatively high glass transition temperature, about 0°C, PP shows brittle behavior at low temperatures. To improve the impact strength at low temperatures,

Correspondence to: C. Wang.

* *Former address:* Department of Chemical Engineering, Yuan-Ze University, Neili, Taiwan.

Contract grant sponsor: National Science Council; contract grant numbers: NSC 83-0405-E-155-002; NSC 84-2216-E-155-003.

Journal of Applied Polymer Science, Vol. 75, 1033–1044 (2000)
 CCC 0021-8995/00/081033-12

PP has been usually blended with different elastomers, such as ethylene–propylene rubber (EPR) and styrene/ethylene–butene/styrene (SEBS) triblock copolymers. Recent developments of dynamic vulcanization of ethylene–propylene–diene rubber (EPDM) with PP by Coran and Patel[8] have made the EPDM/PP TPEs available. In preparation of EPDM/PP TPEs, phase-inverse techniques are generally used to make the minor components (PP) to form the continuous phase by appropriately adjusting the volume and the viscosity ratios of both components. Thus, EPDM rubbers particles with diameters of several micrometers are dispersed in the PP matrix when dynamic vulcanization of 60/40 EPDM/PP blends is carried out.

The physical characterization of EPDM/PP TPEs (Santoprene 201-73), using wide-angle X-ray diffraction, transmission electron microscopy, and differential scanning calorimetry (DSC), was carried out recently by Yang et al.[9] Although EPDM and PP are immiscible in a quiescent state, phase mixing of both is found in EPDM/PP TPEs due to the high shear stresses in the process of dynamic vulcanization. It has been found that a small amount of PP which initially dissolves in the EPDM phase and does not have a chance to diffuse out before the EPDM chains are fully crosslinked is trapped in the rubber particles. Moreover, the sizes of PP crystals in the matrix are reduced because of the presence of a small amount of EPDM which makes the crystallization more difficult. These fragmented PP lamellae may serve as tie points to connect the amorphous PP segments. Young et al.[9] concluded that the excellent strain recovery of EPDM/PP TPEs are due to the presence of these fragmented crystallites. Deformations of EPDM/PP TPEs at high strains were studied by Kikuchi et al.[10] using a finite element simulation method. The preservation of the elasticity of the ligament matrix between EPDM particles is considered to account for the strain recovery as well.

To reveal the structure of EPDM/PP TPEs, Ellul et al.[11] applied scanning transmission electron microscopy to observe the domain morphology of thick samples (about 1 μm). It has been pointed out that the crosslinking density of EPDM plays an important role in reducing the tensile set and increasing the tensile strength of TPEs.[8] Swollen-state ^{13}C-NMR spectroscopy has been successfully applied to estimate the crosslinking densities in EPDM-based TPEs.[11] Recently, a comprehensive review article on the EPDM/PP TPEs prepared by dynamic vulcanization was published.[12]

In this study, investigations concerned with the effects of temperature and the rate on the strength of EPDM/PP TPEs were extensively investigated. Fracture energies were determined using a conventional tear test and a cutting test developed recently.

EXPERIMENTAL

Sample Preparation

The EPDM/PP TPEs, named Santoprene 201-87, were obtained from Advanced Elastomer Systems Co. (Akron, OH). The weight fraction of the EPDM component is 0.52, determined using a xylene solvent to extract the PP component at 135°C. Test samples were prepared using the compression-molding method, first melting at 180°C for 20 min and then cooling in the ambient condition to the room temperature. The final thickness of the EPDM/PP TPE sheets was about 1.0 mm. Thermal properties, including the glass transition temperature, melting temperature, and crystallinity of the samples were measured using DSC (DuPont 910) with a heating rate of 10°C/min from −100 to 200°C.

Measurements of Fracture Energy

Tear Test

The trouser tear test was carried out to determine the tear strength of the EPDM/PP TPE. This tear strength is considered to represent the fracture energy, G_c. To prevent a tear deviation, the strip samples, 100 × 20 × 1 mm, was scored on one side with a razor blade along the centerline to a thickness of 0.7 mm. Thus, about 0.3 mm of the thickness remained to be torn through. The fracture energy, G_c, is calculated using eq. (1):

$$G_c = 2\lambda f/t \tag{1}$$

where λ is the extension ratio of the tear legs; f, the force to propagate a tear; and t, the torn thickness. A schematic representation of the tear test is shown in Figure 1. Measurements of the fracture energies were carried out at various temperatures (25–150°C) and at different tearing rates: R = 8.3 μm/s to 8.3 mm/s. Each experimental result was an average of five tear tests. The fracture surface of the torn samples was ex-

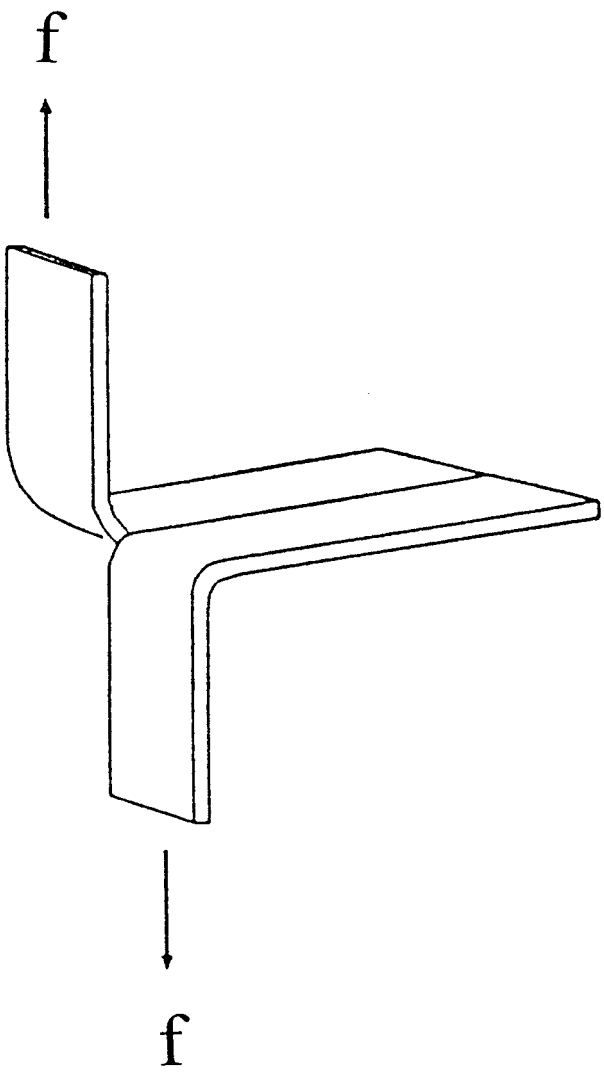

Figure 1 Schematic representation of a tear test.

amined using a scanning electron microscope (SEM, Topon ABT-60).

Cutting Test

In the cutting test, a sharp blade is applied to cut through materials. Previous studies[13–16] showed that the measured fracture energy is significantly reduced when a sharp blade is applied at the tip of a crack. This phenomenon was attributed to a constant crack-tip diameter, which equals the sharpness of the blade, in the process of fracture. In a cutting test, the pulling energy P and the cutting energy C are given as follows[15,16]:

$$P = 2\lambda f_A(1 - \cos\theta)/t \quad (2)$$

$$C = \lambda f/t \quad (3)$$

where f is the cutting force; f_A, the pulling weight; t, the cut thickness; and 2θ, the angle between the two legs. Figure 2 shows a schematic sketch of the cutting test. Thus, by measuring the cutting force and the cutting angle, the fracture energy G_c is calculated from the sum of energies expended in both pulling and cutting:

$$G_c = P + C \quad (4)$$

Details of the cutting characteristics were given elsewhere.[6,15] The cutting tests were carried out at various temperatures (25–150°C) and cutting speeds (0.83 μm/s to 0.83 mm/s). Each experimental value of G_c was obtained from at least 12 measurements.

Tensile Properties

The tensile properties of the EPDM/PP TPE were determined using an Instron tensile testing machine equipped with an extensometer. The gauge length was 10 mm and the sample width and thickness were 4 and 0.8 mm, respectively. Tests

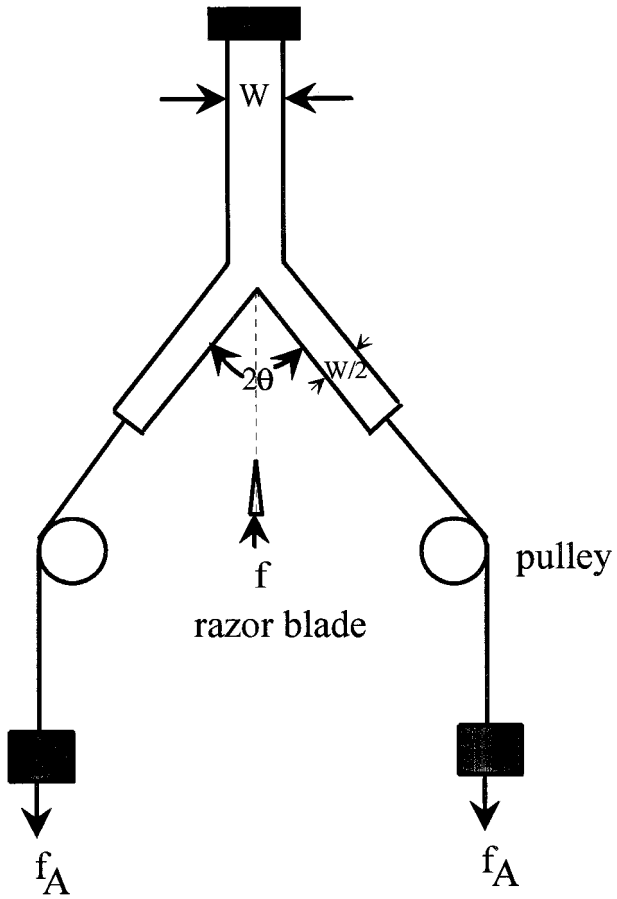

Figure 2 Schematic representation of a cutting test.

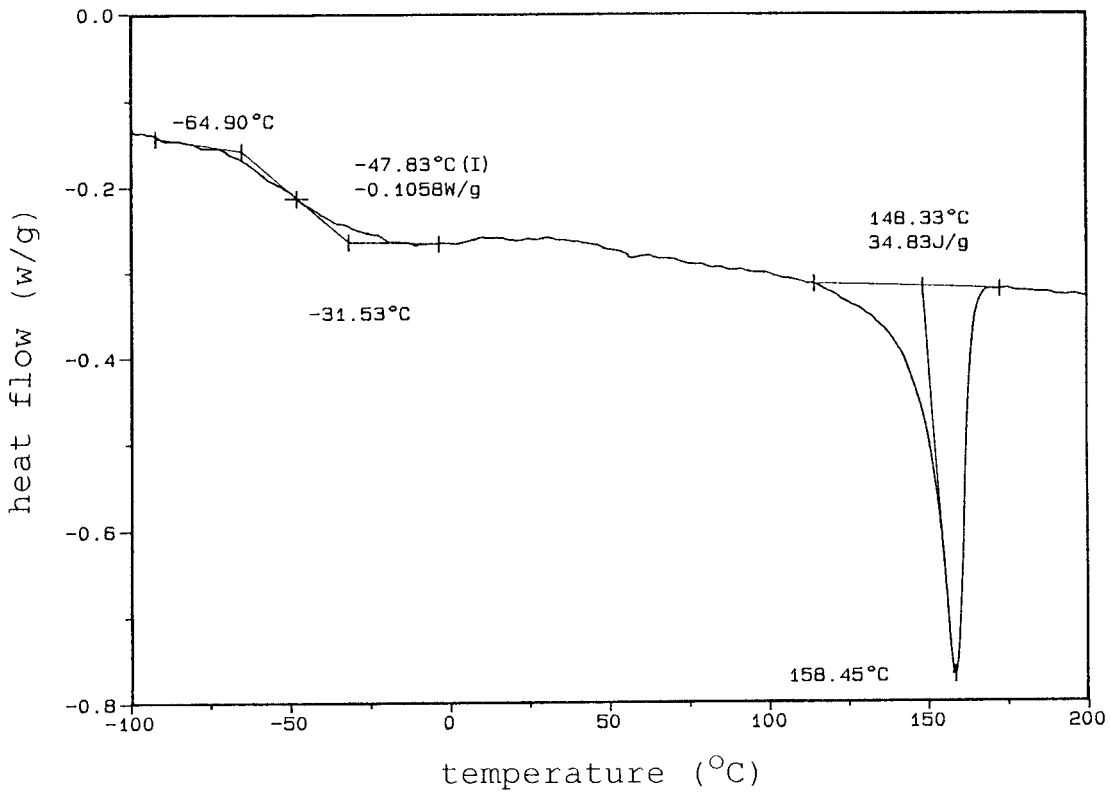

Figure 3 DSC thermograph of the EPDM/PP TPE.

were conducted with various strain rates, $\dot{e}$, at different temperatures (25–80°C). The strain energy density at break, U_b', was determined from the area under the stress–strain curve. The Young's modulus E and breaking stress σ_b were measured as well.

RESULTS AND DISCUSSION

Figure 3 shows the DSC curve of the EPDM/PP TPE at a heating rate of 10°C/min. A broad glass transition temperature, about −47.8°C, of the EPDM phase was observed, whereas the glass transition for the PP phase, about 0°C, revealed by a dynamic mechanical analyzer,[9] is not observed from the DSC thermographs. Moreover, an apparent melting peak is evident at 158.5°C for the PP phase and the onset of melting is 115°C. The crystallinity is about 16.7%, determined from the ratio of the melting enthalpy to the 100% crystalline PP, 209 J/g.

Tearing Characteristics

On tearing the EPDM/PP TPE, two types of failure modes are observed, that is, steady tearing and stick–slip tearing. It seems that steady tearing is the dominant fracture process when the EPDM/PP TPE is torn through. Stick–slip tearing takes place only at high temperatures and low tearing rates, as shown by the filled symbols in the Figure 4. This is in contrast to that for tearing SBS block copolymers which shows stick–slip tearing at room temperature.[6] When stick–slip tearing occurs, the minimum force is used to determine the fracture energy by eq. (1) and the crosshead speed is applied to represent the apparent tearing rate, R. From Figure 4, it is evident that the G_c measured by the tear test decreases when measurements are carried out at high temperatures. Values of G_c are decreased from 10.40 $\pm$ 0.94 kJ/m^2 at room temperature to about 1.87 $\pm$ 0.38 kJ/m^2 at 150°C. On the other hand, the effect of the tearing rate on G_c is negligible when steady tearing takes place. However, an apparent increase in the fracture energy is obtained once the stick–slip phenomenon occurs, as shown in Figure 4.

The exact mechanism to cause the transition from steady to stick–slip tearing is uncertain at present. One possible explanation for the stick–slip tearing is the existence of an anisotropic nature at the crack tip. Gent and Kim[17] showed that

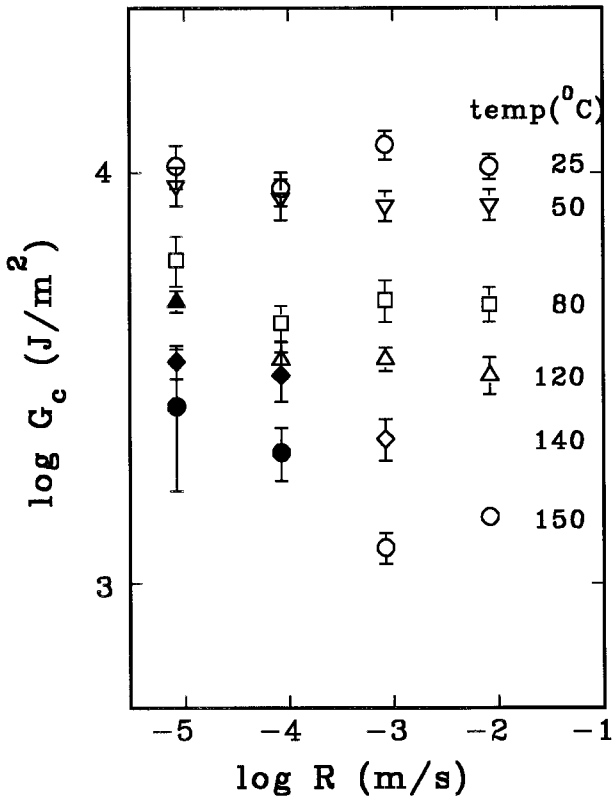

Figure 4 Tear strength, G_C, of EPDM/PP TPE versus tearing rate at different temperatures: (open symbols) steady tearing; (filled symbols) stick–slip tearing.

the measured tear strength of elastomers is higher for a crack to propagate perpendicular to rather than parallel to the predrawn directions. According to Figure 4, the rate–temperature superposition of the tear strength, which was successfully applied to some elastomers,[18,19] seems infeasible for the EPDM/PP TPEs. This is due to the complex interaction between the two phases: the dispersed EPDM particles and the continuous PP matrix.

It has been pointed out that there is a close relation between the fracture energy and the torn surface.[6] A rough torn surface usually accompanies a high fracture energy. Figure 5 shows the SEM micrographs of the fracture surface of samples torn at room temperature. No apparently isolated EPDM particles (domains) or voids are detected. It is evident that small-scale yielding of the PP matrix takes place and features of particle-like protrusion are observed [Fig. 5(b,d)]. The small-scale yielding is attributed to the deformation of the fragmented PP lamellae which are also responsible for the more elastomerlike nature of EPDM/PP TPEs.[9] A rough but uniform torn surface is found [Fig. 5(a,c)], which accounts for both the large fracture energy and the process of steady tearing. Moreover, the roughness of the fracture surface is similar [Fig. 5(b,d)] regardless of the tearing rates applied. It is interesting to note that the dimensions of the particle-like protrusion or the "valley" for the counterpart are 1–3 μm, in a similar order with EPDM domains revealed by TEM.[9] Thus, we expect that the fracture locus is at the interface between the EPDM particles and the PP matrix.

It has been pointed out that partial miscibility of EPDM and PP takes place during dynamic vulcanization due to the elevation of lower critical solution temperature at high shear stresses.[9] Lamellae of PP crystals in the EPDM particles were located near the interface. Thus, the PP molecular chains entangled across the matrix and the dispersed phase contribute to the enhanced interfacial strength. On tearing EPDM/PP TPEs, small-scale yielding of the PP matrix takes place first, although a large-scale yielding is absent from the apparent stress–strain relation. The amorphous PP segments between the fragmented PP lamellae are stretched to a highly extended status. Stress transfer across the interface is effective at this stage due to the presence of PP chains anchored in both phases. Since cavitation in the EPDM phase is not found during tensile deformation,[10] the possible location for crack initiation could be either in the PP matrix or at the interface. In consideration of the stress concentration around the EPDM particles and good elastic (less ductile compared to the neat PP) behavior of PP matrix, breaking of the PP chains across the interface initiates the fracture process. Further propagation of the crack is followed along the interface.

When stick–slip tearing occurs, two different morphologies of the torn surface are repeated along the tear path, as shown in Figure 6(b,c) for the stick and slip regions, respectively. The sample was torn at 150°C and 8.3 μm/s. A relatively smooth and small roughness is observed in the slip region where fast crack growth takes place. However, small-scale yielding of the PP matrix is still observed in the stick region where crack growth is arrested and an increasing tear force is detected. The tear strength at this tearing rate is 2700 $\pm$ 1000 J/m^2. At a higher tearing rate, 8.3 mm/s, a process of steady tearing is observed again, whereas a smaller tear strength is obtained, 1460 $\pm$ 70 J/m^2. Figure 7 shows SEM micrographs of the torn surface. Yielding of the matrix is barely seen and the torn surface is uniform.

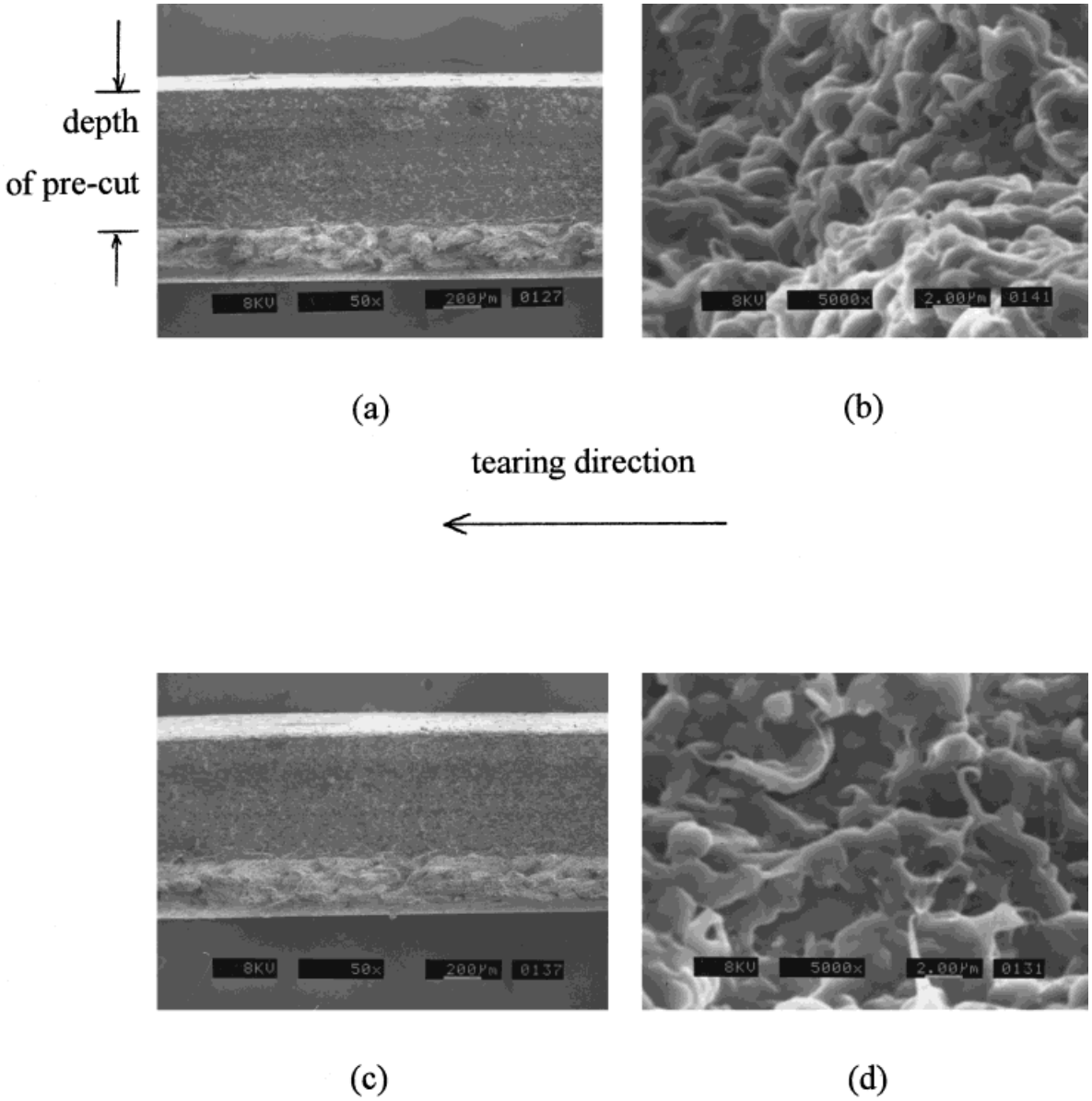

Figure 5 SEM micrographs of specimens torn at $T = 25°C$: (a,b) $R = 8.3$ μm/s; (c,d) $R = 8.3$ mm/s.

Cutting Characteristics

When a fresh blade is used to cut the EPDM/PP TPEs continuously, the sharpness of the blade is gradually reduced. Thus, a larger force is required to cut through the materials, which results in an unexpected increase in the fracture energy. As shown in Figure 8, the fracture energies measured by continuously cutting increase gradually and reach a stable value, about 950 J/m^2, after a cutting length of 15 cm. It implies that, initially, the sharpness of the blade is significantly reduced until a cutting length of 15 cm, where the blade tip diameter holds constant thereafter. A similar phenomenon has also been observed in cutting styrene–butadiene rubbers.[15] However, it is different from that of the cutting of SBS block copolymers, which shows a constant G_c until a critical cutting length is reached where the measured G_c value starts to increase.[6] According to Figure 8, meaningful and reproducible results were obtained only for a fresh blade after cutting a distance of more than 15 cm. In addition, the blade was replaced after being used to cut a distance of 45 cm.

Figure 9 shows the plot of the cutting energy, C, versus the pulling energy, P, at room temper-

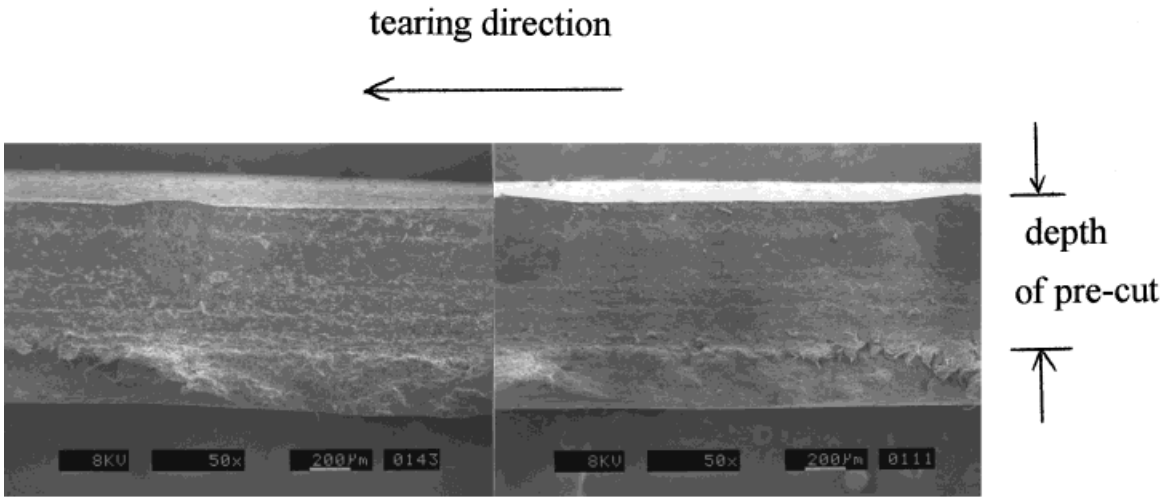

(a)

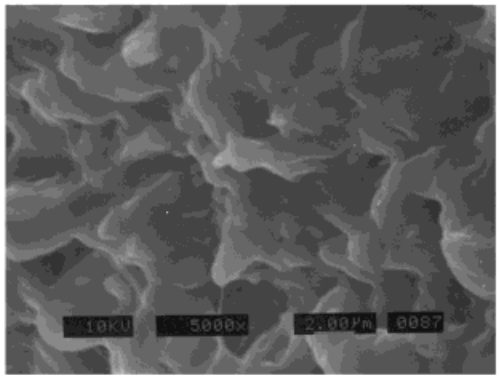

(b)

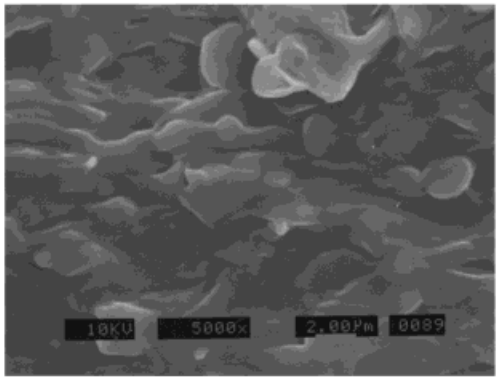

(c)

Figure 6 SEM micrographs of specimens torn at $T = 150°C$ and $R = 8.3$ μm/s where stick–slip tearing occurs; (a) fracture surface of the whole samples; (b) stick region; (c) slip region.

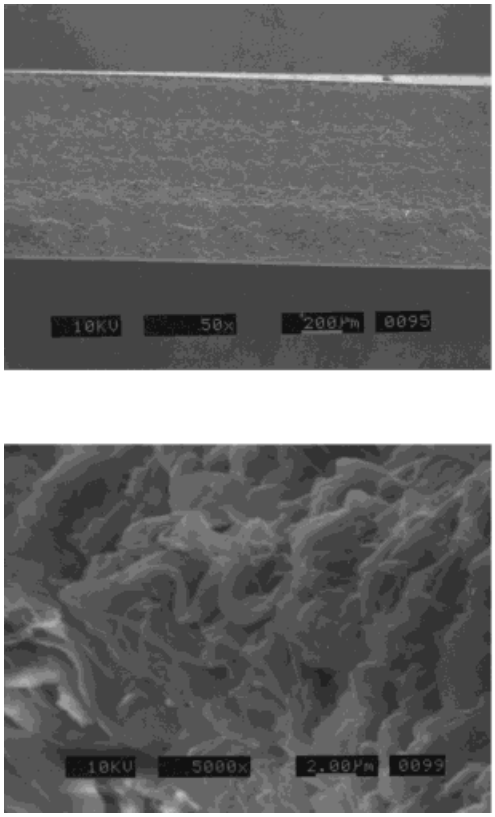

Figure 7 SEM micrographs of specimens torn at T = 150°C and R = 8.3 mm/s where steady tearing occurs: (a) fracture surface of the whole specimen; (b) torn surface.

ature at a rate of 83 μm/s. It should be noted that friction between the razor blade and the sample is evident when the pulling energy is small: P < 100 J/m^2. When silicone oil is applied to the tip

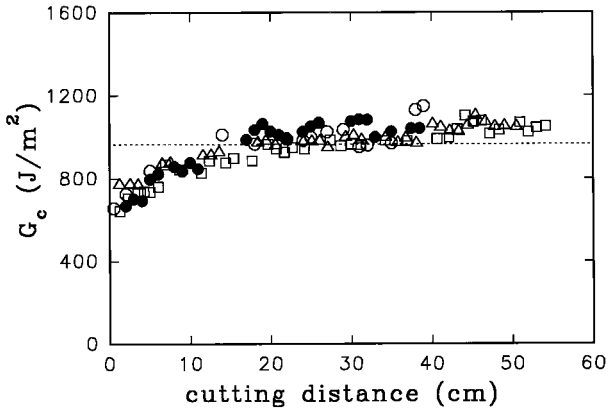

Figure 8 Effect of cutting length on the measured fracture energy; bluntness test of the razor blade: (○) first blade, (△) second blade; (□) third blade; (●) fourth blade.

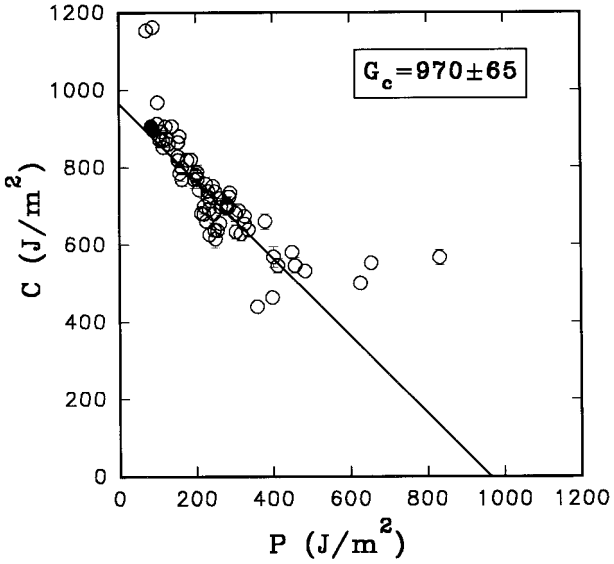

Figure 9 Cutting energy, C, versus pulling energy, P, at T = 25°C and R = 83 μm/s: (filled symbols) with silicone oil applied at the blade tip; (open symbols) without silicone oil.

of the blade, reduction of the friction, shown by the drop of the cutting force and thus the cutting energy, is observed. Similar results have been found in cutting styrene–butadiene rubbers[15] and SBS block copolymers.[6] The details of the plots were discussed elsewhere.[6]

According to eq. (4), the fracture energy is determined from the intercept, about 970 ± 65 J/m^2, by the linear line with a slope of −1 in the region where the pulling energy is smaller than 600 J/m^2. Similar procedures have been conducted on cutting the EPDM/PP TPE at different temperatures and various cutting speeds.

Figure 10 shows the results obtained for samples measured at 150°C and R = 83 μm/s. From the plot, a value of G_c, 910 ± 16 J/m^2, was deduced. Although one-fourth of the PP crystals was melted at 150°C, as shown in Figure 3, insignificant reduction of the G_c is found. Indeed, the effect of temperature on the fracture energy measured by cutting is not pronounced in the temperature range, 25–140°C, as shown in Figure 11. The effect of the cutting speed on the G_c is rather small except at a high temperature where a relatively low G_c is found at a low cutting speed (150°C and 0.83 μm/s). By taking the average of the G_c values at various cutting speeds, the apparent fracture energies at different temperatures were determined and are tabulated in Table I. The G_c values measured by the cutting test decreases slightly from 1000 to 750 J/m^2 for test

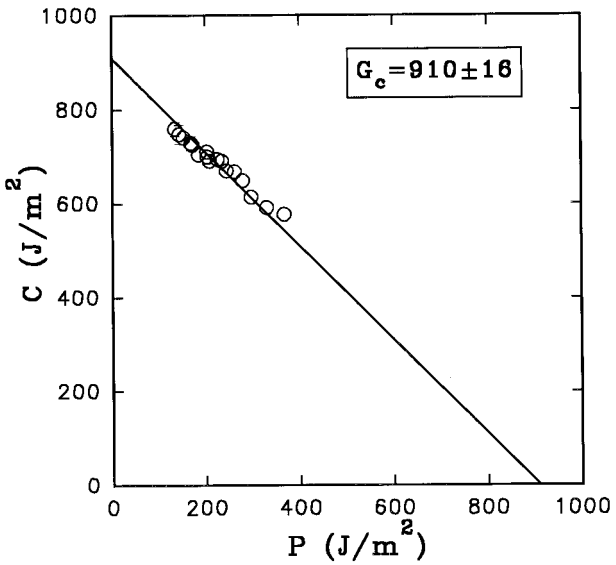

Figure 10 Cutting energy, C, versus pulling energy, P, at T = 150°C and R = 83 μm/s.

temperatures from 25 to 150°C. However, it should be noted that the fracture energy is eventually zero at a temperature higher than 175°C where complete melting of the PP crystals takes place and polymer chains start to flow.

Comparison of G_c Obtained from Tearing and Cutting

In general, the fracture energy determined from the tear test is much higher than that obtained from the cutting test. Table I also shows the variations of the fracture energies obtained from the tear test at different temperatures. The effect of temperature on the measured G_c is more pronounced when a tear test is conducted, from 10,400 to 1340 J/m^2 for test temperatures from 25 to 150°C.

Thomas showed that the fracture energy is quantitatively related to the strain energy density of the materials in the vicinity of the crack tip, as follows[20]:

$$G_c = dU_b \tag{5}$$

where d is the diameter of the crack tip and U_b is the strain energy per unit volume. Thus, the measured fracture energy depends on two factors: One is the strain energy density and the other is the diameter of the crack tip. The former is the intrinsic material properties. The latter, however, is associated with the process of fracture. Therefore, fracture strength can be enhanced when the failure locus is carefully controlled to render a blunt crack tip. "Knotty" tearing is such a fracture process to result in toughness improvement in carbon black-filled elastomers.[21]

On tearing an elastomer, the diameter of the tear tip is found to depend on the tearing rates and temperatures and is in the order of 0.1–1 mm.[15,21] In cutting a material, however, the crack tip diameter induced by a sharp blade is about 0.1 μm, which is determined by the blade tip. Thus, a significant benefit from the cutting test is that a constant d is obtained during the test. Therefore, the intrinsic strength of the EPDM/PP TPEs, U_b, can be determined from the fracture energy measured by the cutting test. In contrast, the fracture energy measured from a tear test is a resultant contribution from both d and U_b.

The intrinsic strength, U_b, of EPDM/PP TPE is calculated to be about 7.4–11.7 GJ/m^3 using a crack-tip diameter of 0.1 μm. It is almost twice larger than that for C—C bond rupture, about 5 GJ/m^3. When tearing is carried out, on the other hand, the tear-tip diameter is estimated to be about 1 μm at room temperature. At 150°C, a sharper crack tip with a diameter about 0.2 μm is deduced.

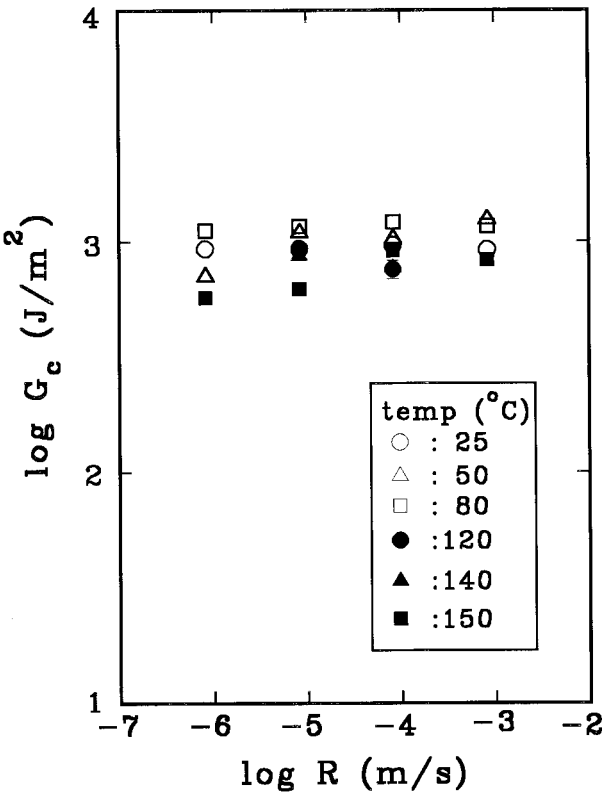

Figure 11 Fracture energy, G_C, determined from cutting test at various rates and temperatures.

Table I Effect of Temperature on Fracture Energies of EPDM/PP TPE Determined from Cutting Test and Tear Test, Respectively, and U_b' Obtained from the Tensile Test

Temperature (°C)	G_c (J/m^2) Cutting	G_c (J/m^2) Tear	U_b' (MJ/m^2)
25	927 ± 30	10,400 ± 940	18.9 ± 2.5
50	1025 ± 230	8660 ± 455	19.7 ± 2.9
80	1170 ± 140	5035 ± 770	22.9 ± 6.4
120	840 ± 115	3655 ± 240	—
140	825 ± 70	2255 ± 150	—
150	735 ± 160	1340 ± 160	—

A comparison of measured G_c values of different polymers from both cutting and tear tests is shown in Table II. It is clear that the fracture energy measured by the cutting test is always smaller than that by the tear test owing to the geometric difference in crack tips. It seems that thermoplastic (LDPE and HDPE) possess higher intrinsic strength, compared with elastomers (silicone and styrene–butadiene rubbers). TPEs (SBS and EPDM/PP) have an intermediate strength because of their possession of plastic and elastomeric characteristics. Further implication is that plastic yielding could be a more effective process for energy dissipation than is simply viscoelastic motion.

Tensile Properties

The effect of strain rate, $\dot{e} = R$/gauge length, on the stress–strain relation of EPDM/PP TPE is shown in Figure 12 at room temperature. When the rate of strain increases, the breaking stress slightly increases but the elongation at break decreases. Figure 13 shows the temperature effect on the stress–strain relation at a constant strain rate, 8.3×10^{-3} 1/s. The elongation at break is found to increase with temperature, from 2.8 at 25°C to 10.0 at 80°C. It should be noted that the crystallinity of PP remains unchanged, as seen from Figure 3, in the temperature range studied. Thus, the pronounced drawability of EPDM/PP TPEs at 80°C is attributed to the pull-out of PP chains from the lamellae crystals. The value of breaking stress, however, is decreased from 8.2 to 4.8 MPa, correspondingly.

The effect of temperature on the Young's modulus, E, and breaking stress, σ_b, is more pronounced than that of the strain rate, as shown in Figures 14 and 15. Generally speaking, the Young's modulus of EPDM/PP TPEs depends mainly on the rigid PP crystals at low strain, whereas breaking stress is associated with the ability of deformation at large strain. As the temperature is increased, the softness of the fragmented PP crystals makes the reinforced effect less pronounced. Indeed, a significant reduction of the Young's modulus is found, from 254 ± 40 to 25 ± 6 MPa, for a temperature from 25 to 80°C. At the corresponding temperature change, the breaking stress is reduced only from 8.3 ± 0.2 to 4.6 ± 0.8 MPa. However, the energy density at break, U_b', determined from the area under the

Table II Fracture Energies of Different Materials Determined from Cutting Test and Tear Test

Polymer	G_c (J/m^2) Cutting	G_c (J/m^2) Tear	Reference
Silicone rubber	70	215 ± 15	16
Styrene–butadiene rubber	190 ± 15	630 ± 30	15
SBS block copolymers	570 ± 20	12,650 ± 650	6
SBS crosslinked with 0.1 phr DCP	375 ± 12	4590 ± 280	6
EPDM/PP TPEs	970 ± 65	10,400 ± 940	This work
LDPE	1000 ± 200	—	16
HDPE	4000 ± 500	—	16

Test conditions: room temperature, 83 μm/s.

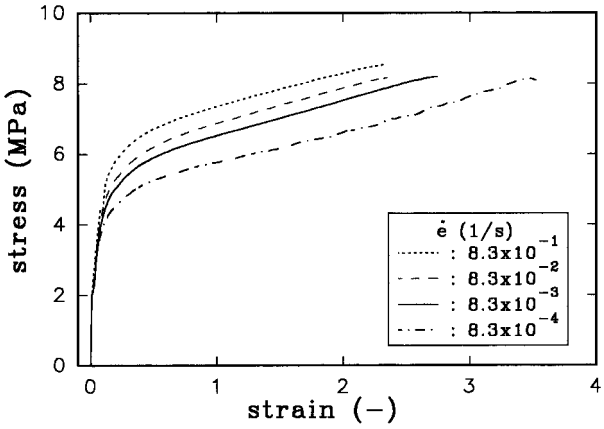

Figure 12 Stress–strain relation of EPDM/PP TPE at different strain rates (room temperature).

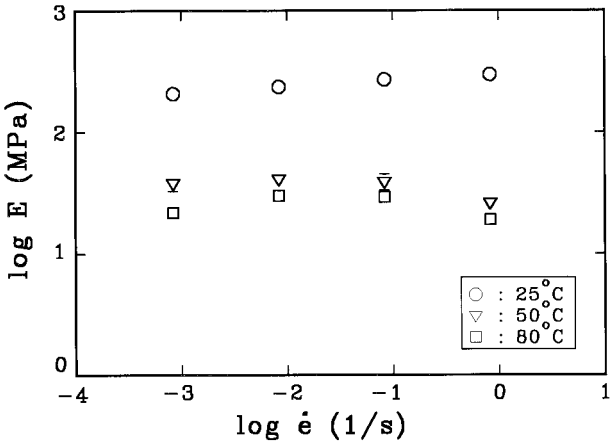

Figure 14 Young's modulus, E, of EPDM/PP TPE versus strain rate at different temperatures.

stress–strain curve, remains more or less constant in spite of the different temperatures and strain rates being used, as shown in Figure 16 and Table I. It is significantly lower than the U_b values, 7.4–11.7 GJ/m^3, determined from the cutting test. It is attributed to the presence of edge flaws in the tensile samples.[15] Of course, the mechanical strength decreases greatly when the temperature is close to the melting temperature of the PP crystals.

CONCLUSIONS

Contribution of the two phases, the continuous PP matrix and the dispersed EPDM particles, to the fracture energy of EPDM/PP TPEs is rather complex. On tearing EPDM/PP TPEs, it seems that steady tearing is the dominant fracture process. The stick–slip fracture process takes place only at high temperatures and low tearing rates. Good tear strength, about 10.40 ± 0.94 kJ/m^2, was found at room temperature. The tear strength decreases with increasing temperature, but a relatively high tear strength, about 1.87 ± 0.38 kJ/m^2, was preserved at 150°C, where a quarter of the PP crystals were already melted. In contrast, the intrinsic strength of the EPDM/PP TPEs determined from the cutting test is varied slightly, 700–1000 J/m^2, over a wide range of temperatures and rates. It seems that EPDM/PP TPE possesses excellent melt strength at high temperatures owing to the interaction of two phases: the presence of small fragmented PP crystals and fully crosslinked EPDM dispersed domains. Above all, good interfacial strength between them is obtained due to the process of dy-

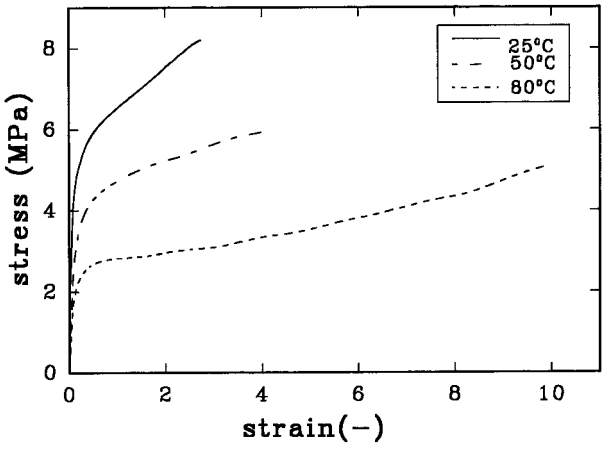

Figure 13 Stress–strain relation of EPDM/PP TPE at different temperatures. Strain rate = 8.3×10^{-3} 1/s.

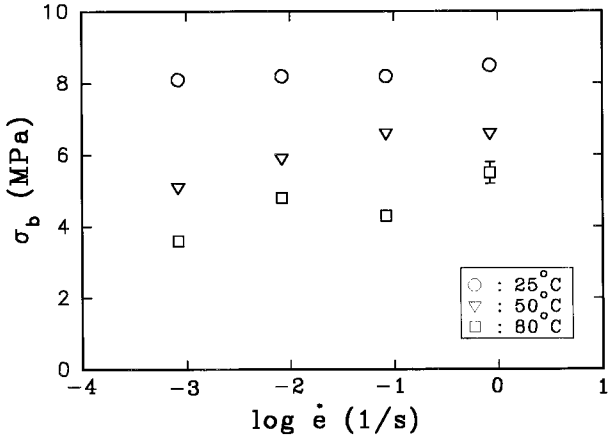

Figure 15 Breaking stress, σ_b, of EPDM/PP TPE versus strain rate at different temperatures.

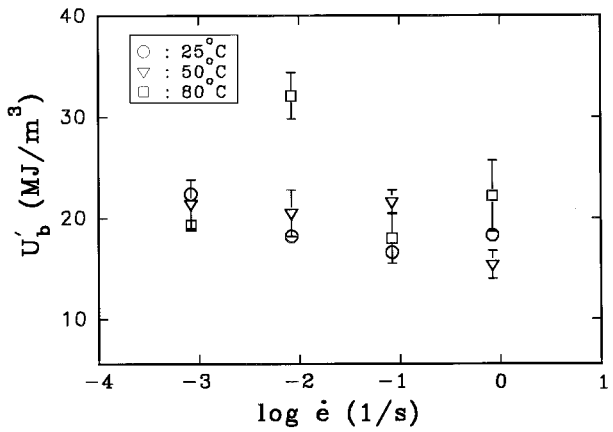

Figure 16 Strain energy density at break, U'_b, of EPDM/PP TPE versus strain rate at different temperatures.

namic vulcanization which promotes the miscibility of PP and EPDM.

The financial support of this work (NSC 83-0405-E-155-002, NSC 84-2216-E-155-003) by the National Science Council is greatly appreciated. The authors are also indebted to Dr. S.-M. Lai at the PIDC for helpful discussions.

REFERENCES

1. Pakula, T.; Saijo, K.; Kawai, H.; Hashimoto, T. Macromolecules 1985, 18, 1294.
2. Séguéla, R.; Prud'homme, J. Macromolecules 1988, 21, 635.
3. Polizzi, S.; Bösecke, P.; Stribeck, N.; Zachmann, H. G.; Zietz, R.; Bordeianu, R. Polymer 1990, 31, 638.
4. Fujimura, M.; Hashimoto, T.; Kawai, H. Rubb Chem Technol 1978, 51, 215.
5. Hashimoto, T.; Fujimura, M.; Saijo, K.; Kawai, H.; Diamant, J.; Shen, M. Adv Chem Ser 1979, 176, 257.
6. Wang, C.; Chang, C.-I. J Polym Sci Polym Phys 1997, 35, 2003.
7. Wang, C.; Chang, C.-I. J Polym Sci Polym Phys 1997, 35, 2017.
8. Coran, A. Y.; Patel, R. Rubb Chem Technol 1980, 53, 141.
9. Yang, Y.; Chiba, T.; Saito, H.; Inoue, T. Polymer 1998, 39, 3365.
10. Kikuchi, Y.; Fukui, T.; Okada, T.; Inoue, T. Polym Eng Sci 1991, 31, 1029.
11. Ellul, M. D.; Patel, J.; Tinker, A. J. Rubb Chem Technol 1995, 68, 573.
12. Abdou-Sabet, S.; Puydak, R. C.; Rader, C. P. Rubb Chem Technol 1996, 69, 476.
13. Lake, G. J.; Yeoh, O. H. J Polym Sci 1987, 25, 1157.
14. Cho, K.; Lee, D. J Polym Sci Polym Phys 1998, 36, 1283.
15. Gent, A. N.; Lai, S.-M.; Nah, C.; Wang, C. Rubb Chem Technol 1994, 67, 610.
16. Gent, A. N.; Wang, C. J Polym Sci Polym Phys 1996, 34, 2231.
17. Gent, A. N.; Kim, H. J. Rubb Chem Technol 1978, 51, 35.
18. Gent, A. N.; Lai, S.-M. J Polym Sci Polym Phys 1994, 32, 1543.
19. Chun, H.; Gent, A. N. Rubb Chem Technol 1996, 69, 577.
20. Thomas, A. G. J Polym Sci 1955, 18, 177.
21. Lake, G. J.; Thomas, A. G. In Engineering with Rubber; How to Design Rubber Components; Gent, A. N., Ed.; Hanser: New York, 1992; Chapter 5.